Medical Microbiology and Immunology (2019) 208:793–809
https://doi.org/10.1007/s00430-019-00628-3

ORIGINAL INVESTIGATION

Role of coaggregation in the pathogenicity and prolonged colonisation of *Vibrio cholerae*

Yien Shin Toh[1] · Soo Ling Yeoh[2] · Ivan Kok Seng Yap[3] · Cindy Shuan Ju Teh[4] · Thin Thin Win[5] · Kwai Lin Thong[2] · Chun Wie Chong[6,7]

Received: 15 January 2019 / Accepted: 19 June 2019 / Published online: 1 July 2019

Abstract

Cholera is an acute diarrheal illness caused by the Gram-negative bacterium *Vibrio cholerae*. The pathogen is known for its ability to form biofilm that confers protection against harsh environmental condition and as part of the colonisation process during infection. Coaggregation is a process that facilitates the formation of biofilm. In a preliminary in vitro study, high coaggregation index and biofilm production were found between *V. cholerae* with human commensals namely *Escherichia coli* and *Enterobacter cloacae*. Building upon these results, the effects of coaggregation were further evaluated using adult BALB/c mouse model. The animal study showed no significant differences in mortality and fluid accumulation ratio between treatment groups infected with *V. cholerae* alone and those infected with coaggregation partnership (*V. cholerae* with *E. coli* or *V. cholerae* with *E. cloacae*). However, mild inflammation was detected in both partnering pairs. Higher density of *V. cholerae* was recovered from faecal samples of mice co-infected with *E. coli* and *V. cholerae* in comparison with other groups at 24 h post-infection. This partnership also elicited slightly higher levels of interleukin-5 (IL-5) and interleukin-10 (IL-10). Nonetheless, the involvement of autoinducer-2 (AI-2) as the signalling molecules in quorum sensing system is not evident in this study. Since *E. coli* is one of the common commensals, our result may suggest the involvement of commensals in cholera development.

Keywords *Vibrio cholerae* · Human commensal · Coaggregation · Adult mouse model

Introduction

Cholera is an acute diarrheal illness that poses a persistent public health problem mainly in developing countries with poor sanitation and lack of clean water supply [1]. Over 1.3–4.0 million incidences and approximately 21,000–143,000 global fatalities are recorded annually, reflecting the prevalence of cholera [2]. Cholera is an intestinal infection caused by the distinct curve, rod-shaped Gram-negative *Vibrio cholerae* [3]. It is clinically characterised by profuse watery diarrhoea, vomiting and leg cramps [4]. The resulting massive fluid loss can lead to severe dehydration and hypovolemic shock, and without proper treatment, death can occur within hours [4].

Edited by: Silja Weßler.

Electronic supplementary material The online version of this article (https://doi.org/10.1007/s00430-019-00628-3) contains supplementary material, which is available to authorized users.

✉ Chun Wie Chong
chongchunwie@gmail.com

[1] School of Postgraduate Studies, International Medical University, Kuala Lumpur, Malaysia

[2] Institute of Biological Sciences, Faculty of Science, University of Malaya, Kuala Lumpur, Malaysia

[3] Sarawak Research and Development Council, Ministry of Education, Science, Technology and Research, Kuching, Sarawak, Malaysia

[4] Department of Medical Microbiology, Faculty of Medicine, University of Malaya, Kuala Lumpur, Malaysia

[5] Pathology Division, School of Medicine, International Medical University, Kuala Lumpur, Malaysia

[6] Department of Life Sciences, School of Pharmacy, International Medical University, Kuala Lumpur, Malaysia

[7] Centre for Translational Research, Institute for Research, Development & Innovation (IRDI), International Medical University, Kuala Lumpur, Malaysia

Most of the cholera outbreaks are attributed by *V. cholerae* serotype O1, which is classified into classical and El Tor biotypes [5, 6]. In comparison with classical biotype, El Tor is less virulent where the related epidemics accounted for lower ratios of symptomatic infections to total infections and higher frequencies of mild or asymptomatic infections [7, 8]. El Tor carriers also excrete bacteria in their stools for a longer time span with an average of 3–5 days, than classical strain carriers who excrete bacteria for an average 1.5 days [9–11].

In Malaysia, sporadic cholera outbreaks are often associated with *V. cholerae* O1 El Tor, but in year 2000 and 2009, a mixed biotype that is El Tor variant had emerged and caused several outbreaks in Malaysia [12, 13]. El Tor variant was also found to cause cholera outbreaks in Asia, Mozambique [14–17] and Haiti [18, 19]. El Tor variant strains contain classical biotype cholera toxin B subunit gene (*ctxB*) in addition to El Tor O1 phenotype and thus, demonstrated greater infectivity [15]. In comparison to classical and El Tor strains, El Tor variant is shown to produce ten times higher amount of cholera toxin and more virulence in rabbit ileal loops [20] and infant mouse cholera model [21], respectively. Patients infected with El Tor variant developed more severe diarrhoea and dehydration due to enhanced chloride ion secretion and intestinal barrier disruption [22]. It is therefore important to determine the pathogenicity of this new variant in causing the disease especially when it acquires cholera toxin from classical biotype in addition to O1 El Tor phenotype, demonstrating enhanced environmental survivability and transmission efficiency [15].

In this study, *V. cholerae* O1 El Tor N16961 was used as the El Tor wild-type reference strain, and *V. cholerae* El Tor 1761 representing the El Tor variant strain which was isolated during the cholera outbreaks in Terengganu between September and December 2009. A vast majority of studies highlighted that naturally occurring biofilms are composed of multispecies communities, but the interactions of *V. cholerae* with other bacterial species in biofilm development are rarely studied. Herein, 26 genetically distinct bacteria were screened for their ability to form coaggregation with *V. cholerae* N16961 and 1761 variant. Interestingly, high coaggregation index and biofilm production were found between *V. cholerae* strains with human commensals namely *Escherichia coli* and *Enterobacter cloacae*. Extending from the in vitro model, we further evaluated the pathogenicity of these single-species cultures and the dual-species partnership (*V. cholerae* with *E. coli* or *E. cloacae*) using an adult mouse model. The severity of the infection was compared based on fluid accumulation ratio, *V. cholerae* cell density in excreted faeces, intestinal histology and host immunological response. Separately, the concentration of autoinducer-2 (AI-2) was determined to estimate the level of cell–cell interactions. Further, the spatial distribution of *V. cholerae* cells in the intestine was observed using confocal scanning electron microscopy.

Materials and methods

Bacterial strains isolation, identification and culture conditions

Vibrio cholerae O1 El Tor (N16961) and *V. cholerae* El Tor variant (VC1761) were obtained from the Laboratory of Biomedical Science and Molecular Microbiology, University of Malaya. VC1761 was previously characterised and identified as El Tor variant by Teh et al. [13].

Environmental bacterial strains used in this study were isolated from freshwater pond and seawater. Water samples were collected and filtered using 0.45 µm pore size polycarbonate membrane filters. The filtrate was then plated directly onto Luria–Bertani (LB) agar and CHROMagar Orientation (CHROMagar, France), and enriched in alkaline peptone water, pH 8.0 at 37 °C with agitation (150 rpm) for overnight before plated on thiosulfate–citrate–bile salts–sucrose (TCBS) agar for 24 h at 37 °C. All isolated bacterial strains and the two *V. cholerae* strains were maintained and grown on LB medium at 37 °C. All presumptive bacteria isolates which showed distinctive colony morphology on CHROMagar and TCBS were identified by 16S rRNA gene sequencing using forward primer 27F (5′-GAGTTTGATCMTGGCTCAG-3′) and reverse primer 1492R (5′-TACGGYTACCTTGTTACG ACTT-3′).

Construction of phylogenetic tree

The 16S rRNA gene sequences identity of the presumptive isolates was obtained using the basic local alignment search tool (BLAST) (https://www.ncbi.nlm.nih.gov/BLAST/). A neighbour joining phylogenetic tree was constructed using MEGA version 6 software [23] (Fig. S1).

Auto- and coaggregation assay

All initial bacterial suspension (IBS) used were adjusted to the optical density OD_{600} 0.5. Based on the growth curve constructed previously, OD_{600} 0.5 falls in the exponential growth phase of *V. cholerae*. The preparation of IBS was carried out as according to procedure reported by Malik et al. [24]. The auto- and coaggregation partnerships were studied semi-quantitatively using spectrophotometric method [24]. This assay was carried out in triplicates and repeated twice for confirmation. The autoaggregation and coaggregation indices were calculated based on the following equation:

$$\% \text{ aggregation indices} = \left[OD_{660}(\text{total}) - OD_{660}(\text{supernatant})/OD_{660}(\text{total})\right] \times 100,$$

where OD_{660} (total) represents the initial OD_{660} recorded immediately after the related strains were paired; OD_{660} (supernatant) represents OD of the supernatant when the mixture was centrifuged after 2 min. Isolate or pair of isolates that showed score lower than 50% are regarded as weak aggregator, 50–80% as moderate aggregator and > 80% as strong aggregator.

The coaggregation ability of these 26 isolates with two *V. cholerae* strains (N16961 and VC1761) was examined based on the measurement of the optical density of bacterial suspensions before and after centrifugation at 600×*g*. The ability to form autoaggregation was assessed for all 28 isolates, spanning 10 distinct genera (Table 1, Fig. S1).

Crystal violet assay

The biofilm produced by single bacterial species or the coaggregation partnership was compared using crystal violet assay [25]. Briefly, IBS was transferred into 96-well microtiter plate (Orange Scientific, Belgium) and incubated for 24 h. After incubation, the unbounded cells were removed by inversion, followed by vigorous tapping on absorbent paper. Subsequently, adhered cells were heat-fixed in an oven for 15 min at 80 °C. Adhered cells were stained by addition of 125 µL of crystal violet (0.1%) for 15 min at room temperature. The plate was rinsed two times with deionised water, removed by inversion followed by vigorous tapping on absorbent paper to get rid of all excess cells and dye. The microtiter plate was heat-fixed in an oven overnight. Each well of the microtiter plate was added with 125 µL of dimethyl sulfoxide (DMSO) (Fisher Scientific, US) to solubilise the crystal violet. The absorption of the eluted stain was measured at wavelength 595 nm, with sterile broth as blank. This assay was repeated using three biological replicates, each with six technical replicates. The classification of biofilm producer is shown in Table 2.

Table 1 Identification of bacterial isolates by alignment with 16S rRNA gene sequences of organisms in the EMBL database

Isolates	BLAST result/proposed identity	Accession no.	Sequence length (bp)	Identity (%)	Origin
N16961	*Vibrio cholerae* O1 biovar El Tor str. N16961	NR074810	1328	99	Reference strain
VC1761	*Vibrio cholerae* strain VC1761	JN836450	1266	100	Reference strain
BA4	*Bacillus thuringiensis*	KJ542769	1356	100	Seawater
BA5	*Bacillus* sp.	KF956680	1278	100	Lakewater
BA6	*Bacillus* sp.	KF010352	1356	99	Lakewater
EC	*Enterobacter cloacae*	KF254602	1317	100	Seawater
EC3	*Enterobacter ludwigii*	KC139444	1267	96	Lakewater
ECOLI	*Escherichia coli* O145:H28	CP007136	1268	100	Human
HV2	*Halomonas venusta*	KF933652	1345	100	Seawater
KP1	*Klebsiella pneumoniae*	KJ806418	1339	99	Seawater
KP2	*Klebsiella pneumoniae*	J490057	1376	99	Seawater
LY4	*Lysinibacillus* sp.	CP006837	1349	100	Seawater
MC2	*Micrococcus luteus*	KF733697	1311	99	Seawater
PR	*Proteus* sp.	HQ246303	1271	100	Human
PS1	*Pseudomonas* sp.	JQ082145	1336	99	Seawater
PS4	*Pseudomonas otitidis*	JQ659846	1317	99	Seawater
PS6	*Pseudomonas aeruginosa*	KJ612071	1291	100	Human
PS7	*Pseudomonas otitidis*	AB698739	1333	100	Lakewater
PS8	*Pseudomonas* sp.	JX393019	1346	99	Lakewater
PS9	*Pseudomonas* sp.	JQ082145	1293	99	Seawater
SA1	*Salmonella enterica* subsp. *enterica serovar Cubana*	CP006055	1367	100	Human
SA2	*Salmonella enterica* subsp. *enterica serovar Typhimurium*	CP007581	1347	100	Human
SA3	*Salmonella enterica* subsp. *enterica serovar Typhimurium*	JQ694626	1361	99	Human
VC1	*Vibrio cholerae* O1	CP003069	1345	99	Human
VC2	*Vibrio cholerae*	CP001485	1326	100	Human
VC3	*Vibrio cholerae*	KF661543	1308	100	Human
VC4	*Vibrio mimicus*	KJ604709	1252	100	Human
VP	*Vibrio parahaemolyticus* O1:K33	CP006008	1377	100	Seawater

Table 2 Semi-quantitative classification of biofilm production [87]

Formula	Strong (*S*)	Moderate (*M*)	Weak (*W*)	Non-adherent/negative (*N*)
SBF = (AB − CW)/G [88]	≥ 1.10	0.70–1.09	0.35–0.69	< 0.35

SBF specific biofilm formation, *AB* stained attached bacteria, *CW* stained control wells, *G* growth in suspended culture

Establishment of mouse model

Among the *V. cholerae* coaggregation partners, *E. coli* (ECOLI) and *E. cloacae* (EC) which showed high coaggregation index were selected for further evaluation using in vivo model. The bacterial strains were cultured in LB medium under conditions described above. About 4×10^8 CFU/mL (based on the pre-determined OD_{600} versus CFU/mL curve) of *V. cholerae* cells were harvested by centrifugation, washed twice and resuspended in 8.5% (w/v) sodium bicarbonate before intragastrically administered into the mice.

Four-week-old female adult BALB/C mice were purchased from a local supplier (Perniagaan Usaha Cahaya, Selangor, Malaysia). The mice involved in this study were marked for identification and kept in individually ventilated cages in animal house facility in International Medical University, Kuala Lumpur, Malaysia. Mice were given ad libitum access to commercial feed and water under controlled environmental conditions (temperature of 25–28 °C, humidity of 60–70%, day/night cycle of 12/12 h). In order to establish a sterile environment for the mice, all cages, bedding, rodent feed and water were either UV radiated or autoclaved prior to usage.

Eleven groups of six BALB/c mice each were used in the experiment, each with different treatments (Table 3). The mice were acclimatised for 7 days before the study was conducted.

On day 5 of acclimatisation, one dose of 0.3% (w/v) penicillin–streptomycin was intragastrically administered to the mice to ablate the gut microbiota. Twenty-four hours before bacterial inoculation, foods were removed from the cage to empty the stomach of the animal. On the day of treatment, one or two doses of 0.3 mL bacterial suspension containing 4×10^8 CFU/mL bacterial cells dissolved in 8.5% (w/v) sodium bicarbonate each were given orally to the animals. The bacterial suspension was prepared according to the group-specific bacterial species combination listed in Table 3. The first dose was given in the morning, followed by the second dose, 6 h after the initial administration. The placebo, which was used in the control group, consisted of only sodium bicarbonate. Sodium bicarbonate was used as a carrier medium to neutralise gastric acid and to increase the chances of successful infection. The mice were kept in cages with free access to food and water after the two doses were administered.

Table 3 Groupings of BALB/c mice subjected to different treatments

Groupings	Treatments	
	First dosage	Second dosage
Control group		
Group 1	Placebo	
Group 2	Placebo	N16961
Group 3	Placebo	VC1761
Group 4	N16961	
Group 5	VC1761	
Group 6	ECOLI	
Group 7	EC	
Co-infection group		
Group 8	ECOLI	N16961
Group 9	EC	N16961
Group 10	ECOLI	VC1761
Group 11	EC	VC1761

Faecal samples were collected before the intestinal inoculation (T0) and at 24, 48 and 72 h post-infection (T24, T48 and T72). The whole body weight of mice was measured after each faecal sampling using a weighing balance (Precisa, Switzerland). At T72, the mice were euthanised by cardiac puncture. The entire stomach and intestines were removed and weighed using a weighing balance to the nearest 0.01 g. The harvested small intestine was trisected by length into proximal, medial and distal segments. The central 1 cm of distal segments were excised for histological analysis. The faecal samples and tissue sections were stored at − 20 °C and − 80 °C, respectively, until further analyses.

Determination of fluid accumulation (FA) ratio

The FA ratio was determined using the calculation formula as follows: weight of stomach plus intestines/(total body weight − weight of stomach plus intestines) [26].

Faecal DNA extraction

Genomic DNA was extracted using QIAamp Fast DNA Stool Mini Kit (Qiagen, Germany). About 0.02 g of faecal samples were weighed and subjected to DNA extraction according to the manufacturer's instructions.

Generation of standard curves and real-time PCR

Vibrio cholerae N16961 and VC1761 were cultured on LB medium under conditions described above. Both *V. cholerae*

were grown to the log phase and the bacterial suspension was serially diluted. The dilutions were plated on LB agar to enumerate the colony forming unit (CFU).

The dilutions were also subjected to DNA extraction using G-spin Total DNA Extraction Kit (iNtRON Biotechnology, Korea). The DNA was quantified under quantitative real-time PCR (qPCR) using primers 5′-ACTCACCACCAG AGGTAGAAATCTT-3′ and 5′-AACGCTTGGCTATAT GTTTACTGACA-3′ that targets *V. cholerae* outer membrane protein (*ompW*). The TaqMan probe used (5′-6FAM-TAGCAGCGAGGACTTC-MGB-NFQ-3′) was labelled with fluorescence dye, phosphoramidite fluorochrome 6-carboxyfluorescein (FAM) at 5′ end. Every 20 µL of qPCR reaction mixture contained 10 µL of TaqMan Universal PCR 2× Master Mix (Applied Biosystems, US), 0.44 µL of each primer and probe (10 µM), 6.68 µL of DNA template as well as 2 µL of nuclease-free water. These reaction mixtures were then subjected to PCR amplification using the CFX96 Touch™ Real-Time PCR Detection System (Bio-rad Laboratories Inc., USA). An initial holding duration of 2 min at 50 °C was set to activate the No Amp Erase UNG and a second holding duration at 95 °C for 10 min to activate AmpliTaq Gold DNA Polymerase, followed by 40 cycles of 95 °C for 15 s and 60 °C for 1 min. C_t values of the amplicons at different dilutions were plotted against the CFU to form a standard curve. The same PCR conditions were used for all faecal DNA samples. The bacterial load in the faecal samples was determined based on the standard curve.

Cytokine multiplex assay

Bio-Plex Cell Lysis Kit (Bio-Rad Laboratories Inc., USA) was used to lyse the intestinal tissue samples. Prior to cytokine multiplex assay, the protein concentration of the tissue lysate was determined using the Bradford method and adjusted to the concentration of 350 µg/mL using Bio-Plex sample diluent containing 0.5% final (w/v) bovine serum albumin (BSA). The cytokine multiplex assay was performed using the customised Bio-Plex Pro Mouse Cytokine 8-Plex Immunoassay (Bio-rad Laboratories Inc., USA) targeted for GM-CSF, IFN-γ, IL-1β, IL-2, IL-4, IL-5, IL-10 and TNF-α. The experimental procedures were carried out according to the manufacturer's instruction. Luminex 200 instrument with the Luminex xPONENT Software (Luminex, USA) was used to detect the fluorophores' signal.

Vibrio harveyi BB170 bioluminescence assay

In this assay, *V. harveyi* BB170 (ATCC BAA-1117) detects AI-2 while *V. harveyi* strains BB152 (ATCC BAA-1119) is a producer of AI-2, acting as a positive control. Both *V. harveyi* strains were cultured in a modified autoinducer bioassay (AB) medium. The AB basic medium contains 17.5 g of sodium chloride (Merck, Germany), 12.3 g of magnesium sulphate (R&M Chemicals, UK) and 2.0 g of casamino acid (Sigma Aldrich, USA). The solution was autoclaved at 121 °C for 15 min. After the solution was cooled to ambient temperature, the following components were added from sterile stocks: 10 mL of glycerol (Friendemann Schmidt Chemical, USA), 10 mL of potassium phosphate buffer pH 7 (Sigma Aldrich, USA) and 10 mL of 0.1 M L-arginine (Sigma Aldrich, USA). In preparation for *V. harveyi* BB170 bioluminescence assay, *V. harveyi* BB152 and *V. harveyi* BB170 were cultured in AB medium for 15 h, with aeration (150 rpm) at 30 °C. The cultivated *V. harveyi* BB152 and *V. harveyi* BB170 were diluted 1:300 in fresh AB medium and stored frozen at − 80 °C until used.

Approximately 15 mg of the harvested intestinal tissue samples were mixed with 500 µL of sterile water. The mixtures were homogenised thoroughly using the tissue homogeniser (Nippi Inc., Japan), and sonicated at 30% amplitude for 2 × 30 s. The lysed samples were subsequently centrifuged at 7000*g* for 4 min. The resulted supernatant was filtered through 0.45 µm Minisart regenerated cellulose filter unit (Sartorius, USA). Cell-free extracts were stored immediately at − 80 °C for future use. For this assay, the cell-free extracts were added to the diluted *V. harveyi* cultures to a final concentration of 10% (v/v) into each well of UV-sterile 96-well black, opaque microtiter plate. The microtiter plate was covered and incubated at 30 °C with aeration (150 rpm). The level of light emission was measured after 6, 10, 16 and 24 h of incubation using Panomics luminometer (Affymetrix, USA). Bioluminescence relative to sterile water was calculated as fold inductions.

Histological examination of mouse intestine

The central 1 cm distal intestinal segments were fixed in 10% neutral buffered formalin for 24 h prior to tissue processing. The processed tissue was embedded, sectioned and stained with hematoxylin and eosin (H&E) (Sigma Aldrich, USA) for visualisation under light microscope. Whilst for fluorescence in situ hybridisation (FISH), Histology FISH Accessory Kit K5499 (Dako, Denmark) was used and the procedures were performed according to the manufacturer's instruction. The tissue sections were hybridised in 10 µL solution containing 100 ng of fluorescently labelled FISH probes (IDT DNA Technologies, USA) and SureFISH FFPE Hybridisation Buffer (Dako, Denmark) at 40 °C for 2 h. Probes used in this study were the universal bacterial probe EUB338 5′-GCTGCCTCCCGTAGGAGT-3′ [27] modified at 5′ end with indocarbocyanine dye cy3 and *V. cholerae/mimicus* specific probe Vchomim1276 5′-ACT TTGTGAGATTCGCTCCACCTCG-3′ [28] modified 5′ end with indocarbocyanine dye cy5. These probes were tested for their specificity and control slides with fixed bacterial

cells were included in every FISH experiments. All the prepared slides were examined using confocal laser scanning microscope (CLSM) (Leica, Germany). Images were captured and analysed using Leica application suite (LASX) software (Leica Microsystems, Germany).

Statistical analyses

The data were presented as mean ± standard error (SE) unless otherwise stated in the experiments. Means with a significant difference ($p < 0.05$) were compared using Student's *t* test from SPSS Predictive Analytics software version 18.0 (IBM, US). Analysis of variance (ANOVA) was used to test for significance across grouping. Multivariate analysis of variance based on permutations (PERMANOVA) was used to compare the cytokine profiles.

Results

Autoaggregation and coaggregation partnership for *V. cholerae* O1 El Tor and O1 variant strains

A total of 26 bacterial isolates were isolated from various sources of aquatic samples including lake water from Bukit Jalil, Kuala Lumpur, seawater from Lumut, Perak, seawater from Penang and stool samples from healthy volunteers (Table 1). Out of these 26 isolates, 24 was found to exhibit moderate to strong autoaggregation (51–96.5%) (Fig. 1, Fig. S1). N16961 was found to be a moderate autoaggregator (51%) while VC1761 exhibited low autoaggregation (44.8%). The ability of *V. cholerae* strains (N16971 and VC1761) to form coaggregation with each other, and the remaining 26 isolates (26 × 2 pairing) was also examined spectrophotometrically (Fig. 1). Twenty isolates showed moderate coaggregation (coaggregation score 50–80%) with VC1761 while 18 isolates showed moderate coaggregation with N16961. Overall, the aggregation score for the coaggregation partners involving N16961 was higher than those involving VC1761. In comparison, the coaggregation score for the partnerships involving VC1761 were higher than the autoaggregation score.

Biofilm formation ability of mono- and dual-species *V. cholerae* biofilm

The crystal violet assay showed that seven isolates, including *V. cholerae* N16961 (SBF = 4.472) were strong biofilm producers (Fig. 2). Two isolates such as *Enterobacter cloacae* EC (SBF = 1.078) and *V. cholerae* VC2 (SBF = 0.817) were categorised as moderate biofilm producers while five isolates including *V. cholerae* VC1761 (SBF = 0.97) were considered as weak biofilm producers. In dual-species model, both EC and ECOLI showed significantly higher biofilm production with N16961 and VC1761 than single-species model.

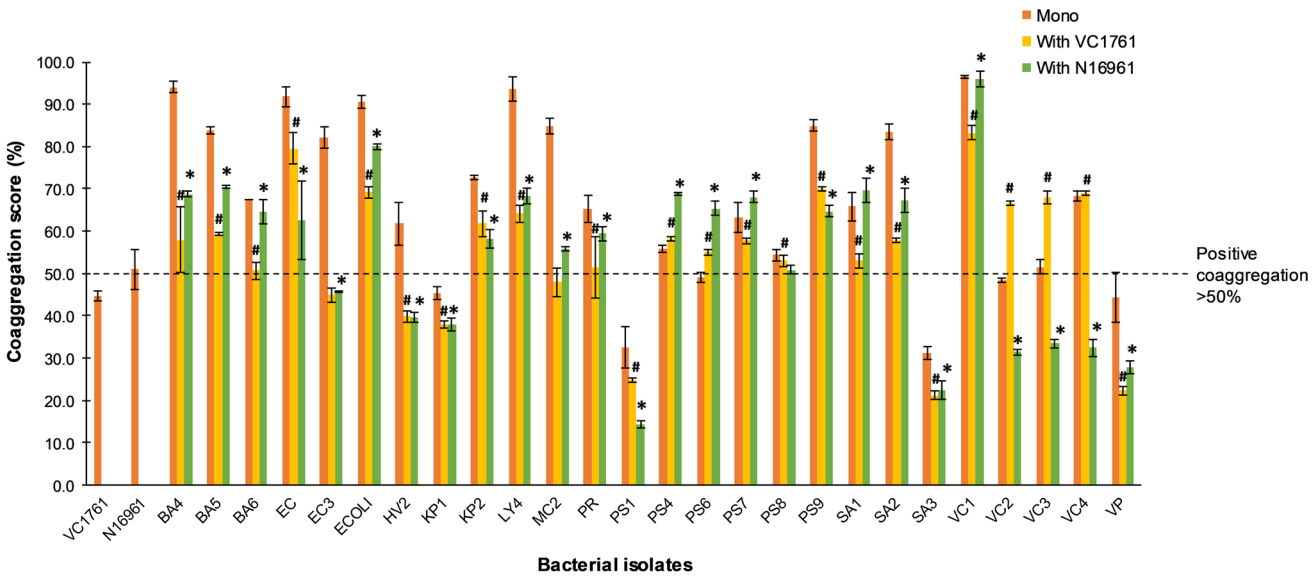

Fig. 1 Results of coaggregation scores (%) between two *V. cholerae* (N16961 and VC1761) with bacterial isolates using coaggregation assay. Bars below the dotted line are considered as weak coaggregation < 50% while above dotted line are considered as positive coaggregation > 50%. Bars represent the mean values with SD. *Significant difference ($p < 0.05$) compared to aggregator N16961. #Significant difference ($p < 0.05$) compared to aggregator VC1761

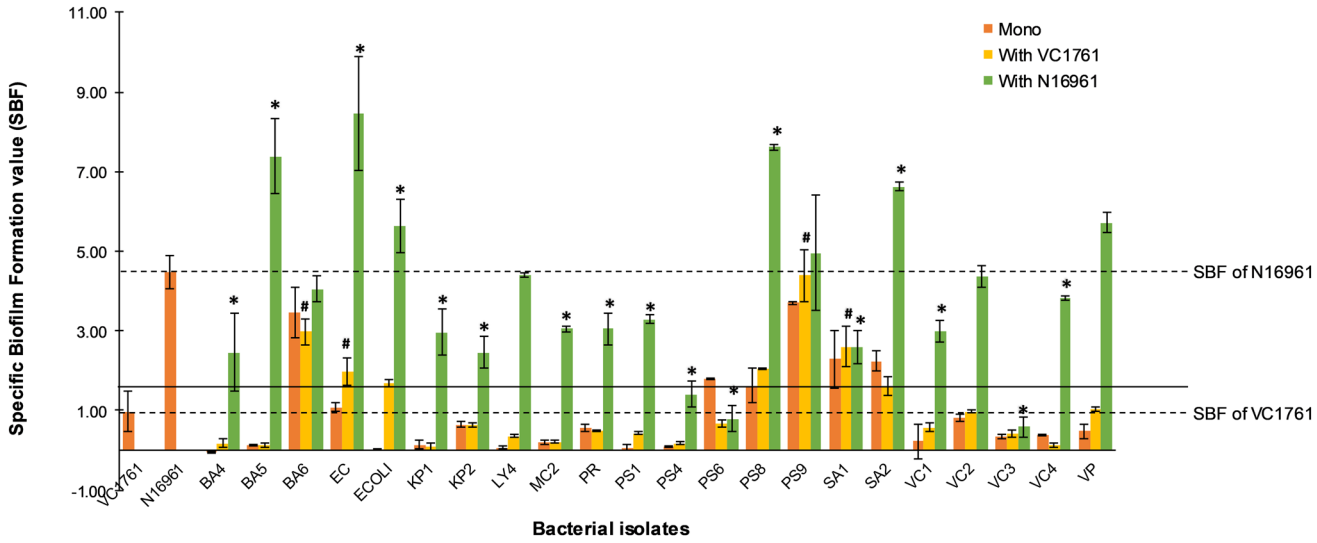

Fig. 2 Biofilm crystal violet assay between two *V. cholerae* (N16961 and VC1761) with bacterial isolates. Upper dotted line considered as N16961 mono-species biofilm while the bottom dotted line considered as VC1761 mono-species biofilm. Bars above the straight line represents strong biofilm producer while bars under straight line represents as moderate, weak or non-adherent biofilm producers. Bars represent the mean values with SD. *Significant difference ($p < 0.050$) of the dual-species biofilm of N16961 compared to N16961 mono-species biofilm. #Significant difference ($p < 0.05$) between the dual-species biofilm of VC1761 compared to VC1761 mono-species biofilm

Establishment of adult mouse model of cholera

Mice were intragastrically administered with or without *V. cholerae* as described previously. Both control mice and co-infected mice did not show significant difference in FA ratio upon termination at T72 (Fig. 3). In addition, all animals showed no signs of diarrhoea. However, the mice co-infected with ECOLI and N16961 showed significantly higher FA ratio compared to mice co-infected with EC and N16961 ($p < 0.05$). Subsequent experiments were performed to further evaluate the effect of coaggregation on the pathogenicity and prolonged colonisation of *V. cholerae*.

Detection of *V. cholerae* using confocal laser scanning microscopy-based fluorescence in situ hybridisation (FISH)

To ascertain whether *V. cholerae* colonised and retained in the intestines, FISH was performed on the distal intestinal segments of all mice infected with *V. cholerae* (single and dual-species mixtures). EUB338 was used as a probe labelling eubacteria (yellow) and Vchomim1276 as a *Vibrio*-specific probe (red). As depicted in Fig. 4, small micro-colonies of *V. cholerae* were detected in all infected mice particularly in the intestinal lumen. In the tissue of control group (placebo), only EUB338 hybridised to the bacteria present in the tissue and no signal was detected when hybridisation with Vchomim1276 was performed.

Histological examination of intestinal tissues after *V. cholerae* infection

The microscopic changes of distal intestinal segments after *V. cholerae* infection were examined via routine hematoxylin and eosin (H&E) staining. Figure 5 shows that intestinal tissues from all the co-infection groups had undergone mild inflammation. In contrast, the control group including groups of mice infected with *V. cholerae* alone, EC alone and ECOLI alone showed no signs of inflammation (Fig. S3). The observed histopathological features in the co-infection group such as mice co-infected with ECOLI and N16961 included a partly degenerated and sloughed ileal mucosa (Fig. 5d). Slight increase in the vascularity in the submucosa (Fig. 5g, h) in mice of co-infection group ECOLI and VC1761 was also detected.

Recovery of *V. cholerae* cells from faecal pellets

Both *V. cholerae* N16961 and VC1761 were detected in faecal pellets of all *V. cholerae*-infected mice (single-species infection and co-infection) at 24 h post-infection. This affirmed that the administered *V. cholerae* was capable of colonising the intestine of our adult mouse model of cholera despite the insignificant FA ratio shown. The total number of recoverable *V. cholerae* was approximately 40-fold higher in the co-infection group consisted of ECOLI and N16961 than that of EC and N16961 ($p < 0.05$) (Fig. 6). Similar trend

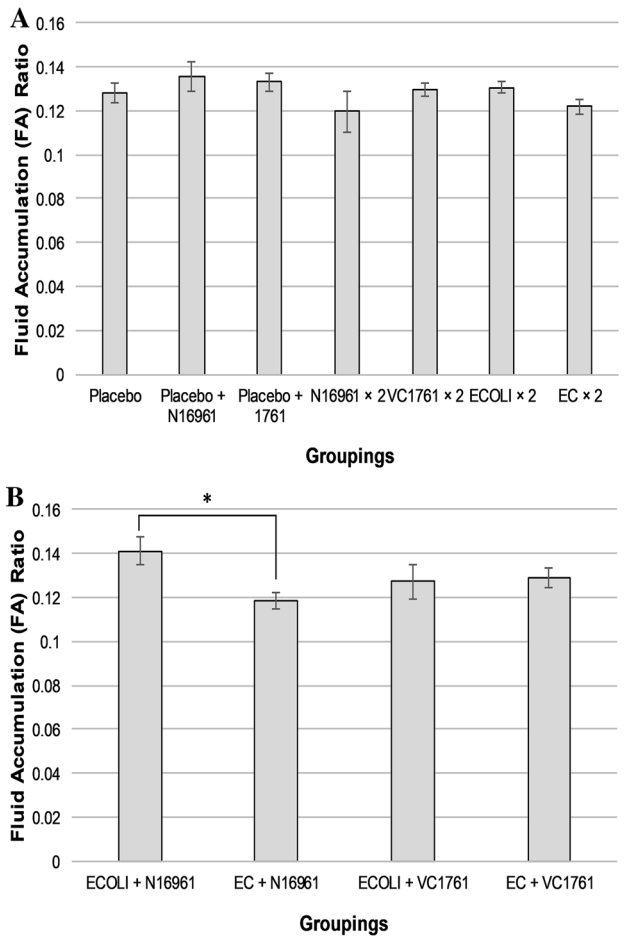

Fig. 3 The FA ratio of mice from the **a** control group (means of six mice) and **b** co-infection group (means of six mice). The FA ratio was calculated as intestinal weight/(whole body weight − intestinal weight). Data represent mean ± SE Student's *t* test, $*p < 0.05$

was observed in mice co-infected with VC1761, but the significant difference was not apparent. *V. cholerae* signal was below detection limit at 48 and 72 h post-infection.

Host immunological response

The targeted cytokines GM-CSF, IFN-γ, IL-1β, IL-2, IL-5, IL-10 and TNF-α were detected in all co-infection groups. Relatively higher IL-5 and IL-10 were detected in the *V. cholerae* (both N16961 and VC1761) and ECOLI partnership than *V. cholerae* with EC (Fig. 7). The significant difference was not apparent.

AI-2 production in coaggregating partnership

To gain insights on the interaction of the coaggregating partnership, *V. harveyi* BB170 bioluminescence assay was performed to analyse the AI-2 (furanosyl borate diester 3A-methyl-5,6-dihydro-furo (2,3-D) (1,3,2) diox-aborole-2,2,6,6A-tetraol) activity produced. Analysis of the cell-free extracts of the homogenised intestinal samples indicated that low levels of AI-2 was observed during the 6-h time point (T6) but high AI-2 at 24-h time point (T24) in all infection groups. The differences in AI-2 accumulated between group of N16961 alone is significantly higher when compared to VC1761 ($p < 0.05$). But, the differences elicited by the dual-species infection in both *V. cholerae* strains is comparable or lower than single-species infection (Fig. 8).

Discussion

Coaggregation ability of *V. cholerae* with other bacterial isolates

To our best knowledge, the coaggregation partnership for *V. cholerae* has not been extensively studied. To increase the coverage of the screening and to increase the chances of finding the potential coaggregation partners, we evaluated the coaggregation ability of two reference strains, N16961 and VC1761 with isolates retrieved from both environmental and stool samples from apparently healthy human volunteers. To avoid the qualitative nature of visual assay, we have adapted a well-accepted spectrometry method [24] for coaggregation screening [29–31].

Based on the coaggregation assay conducted, 22 out of 26 (84.6%) of the isolates were able to positively coaggregate with at least one strains of *V. cholerae* (N16961 and VC1761) (coaggregation score > 50%). Majority of the coaggregation partnerships for N16961 and VC1761 were established with faecal isolates, suggesting the importance of coaggregation in gut colonisation which is mediated by lectin adhesins [32], complementary polysaccharides [33] and lectin–carbohydrate interaction [34, 35]. Intergeneric and intrageneric coaggregation are common phenomenon for freshwater, oral and gut bacteria [35, 36]. However, contrasting ability of intraspecies coaggregation was detected for N16961 and VC1761. For the former, coaggregation was absent for most of the *V. cholerae* strains tested except VC1 while VC1761 was capable to coaggregate with all four *V. cholerae* strains (VC1, VC2, VC3 and VC4). Both VC1761 and N16961 were also not able to form coaggregation with VP. The lack of coaggregation with taxonomically related strains was previously observed for *Blastomonas natatoria* 2.4 which coaggregates poorly with other *Blastomonas* strains [37].

Here, we detected a highly strain-specific coaggregation partnership for N16961 and VC1761 (Fig. S1). For instance, different strains of *Pseudomonas* and *Klebsiella* formed coaggregation with VC1761 and N16961. It is possible that the strain-specific coaggregation of N16961 and

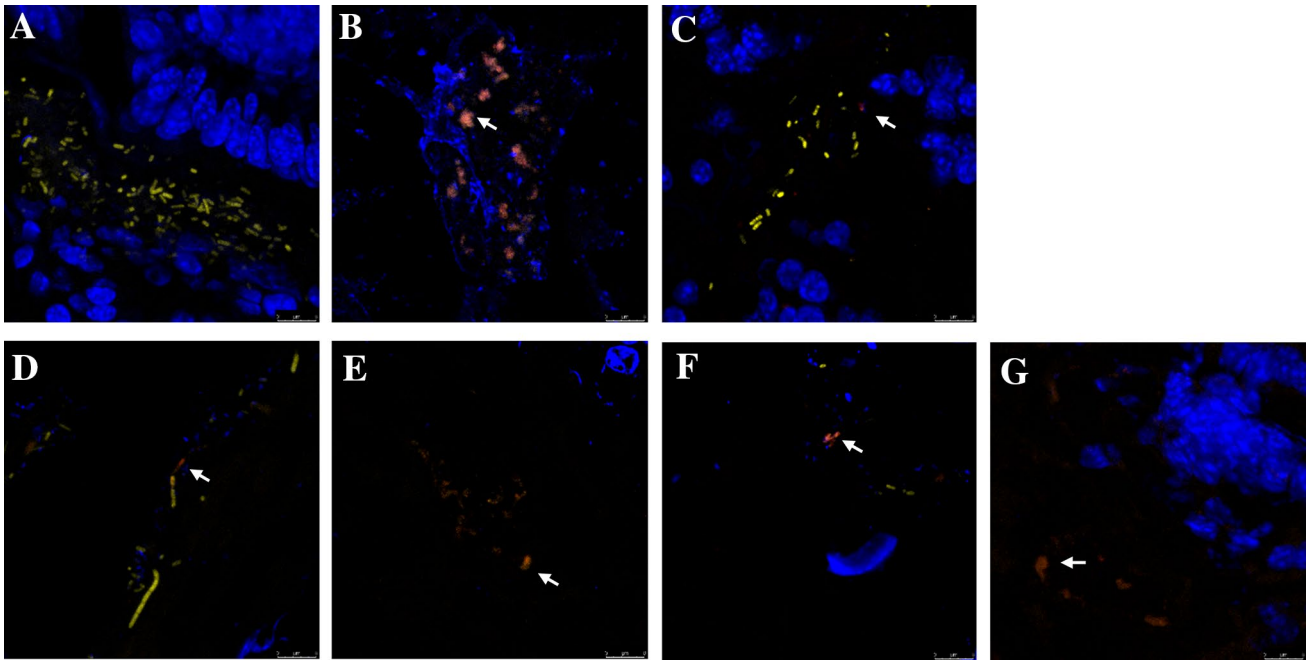

Fig. 4 Detection of fluorescence-labelled *V. cholerae* (as indicated by white arrow) in small intestine by confocal laser scanning microscopy. No *V. cholerae* was present in **a** placebo group but were found in **b** placebo and N16961, **c** placebo and VC1761, **d** EC and N16961, **e** ECOLI and N16961, **f** EC and VC1761, **g** ECOLI and VC1761. Images were taken at 252× magnification. Scale bar = 8 µm. Bacterial cells showing yellow fluorescence were stained by universal bacterial probe EUB338. *Vibrio cholerae* cells were stained by both EUB338 and *Vibrio cholerae/mimicus* specific probe Vchomim1276 and displayed orange fluorescence. Scale bar = 25 µm

VC1761 is mediated by different adhesin and interaction of saccharide receptor between cell surface molecules on partner organisms. It is understood that *V. cholerae* carries adhesin including flagellum, Mam7, GbpA, OmpU, and FrhA [38]. Further studies are required for the identification of specific adhesins of *V. cholerae* that are responsible for "partner" recognition. In addition, strain-dependent interaction might be mediated by specific environmental trigger such as ionic strength of the culture medium, temperature, pH, viscosity and the amount of autoinducer-2 signalling present [39, 40]. Nonetheless, previous report suggested that coaggregation of freshwater bacteria is growth-phase-dependent (maximum at early stationary phase) [32]. It is important to highlight that 16S rRNA gene is not the ideal gene to resolve strain-level differences. Nevertheless, our result affirmed the presence of specific interaction within isolates of the same species.

Autoaggregation had attracted much attention in biofouling in recent years due to its association with production of exopolysaccharides, curli expression, and biofilm promotion [36]. However, unlike coaggregation, autoaggregation is a "self-centred" cell–cell interaction whereby a strain within the biofilm expressed its polymers to improve the integration of genetically identical strains into biofilms [41, 42]. From the 28 isolates tested in the current study, 85.7% displayed positive autoaggregation reactions with aggregation scores ranging from 51 to 96.5% slightly higher than the scores obtained for coaggregation (50–80%) (Fig. 2).

Mono- and dual-species *V. cholerae* biofilm

In nature, mixed-species biofilms dominate in most of the environments [43]. *V. cholerae* are able to promote multi-species biofilm development through cell–cell interaction such as quorum sensing [44, 45]. From the crystal violet assay, we showed that isolates with high coaggregation index (e.g. *Bacillus* sp., *E. cloacae*, *E. coli* isolate, *Pseudomonas* sp. and *S. enterica*) (Fig. 1) were able to enhance the production of biofilm production in partnership with N16961 or VC1761 (Fig. 2). This finding is significant as although planktonic pathogenic *V. cholerae* are able to attach to the mucous coat and along the villous axis of the intestinal mucosa of human and animal models in the form of patches and clonal microcolonies [46, 47], biofilm-derived cells are capable of infecting the small intestinal in lower infective dose, even in the presence of limiting nutrients condition [48].

Among the *V. cholerae*'s coaggregation partners, EC and ECOLI were selected for further evaluation using an adult mouse model because of its stronger synergetic effects in biofilm production (Fig. 2). Although the infection did not induce significant fluid accumulation, the presence of *V.*

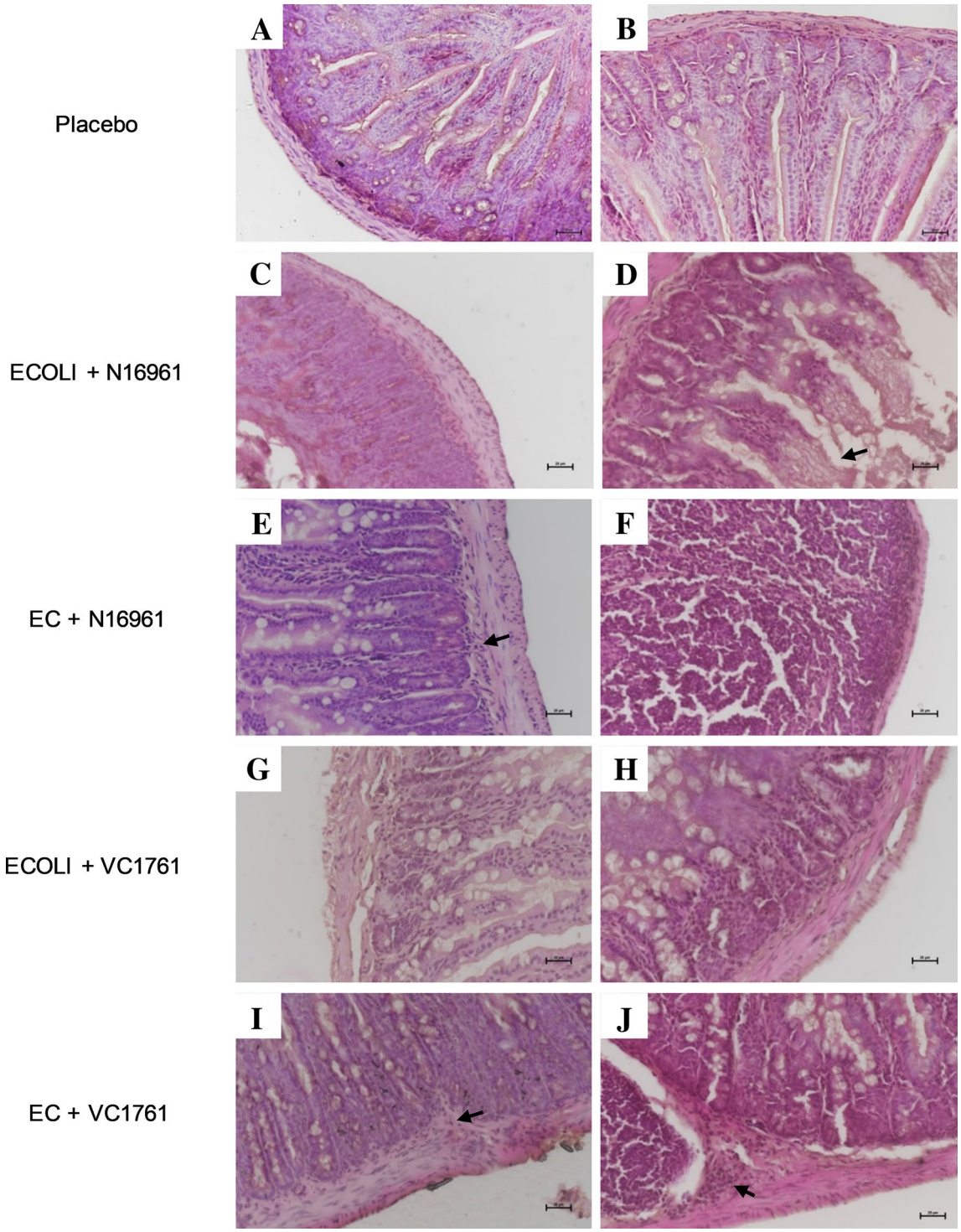

Fig. 5 Representative images of H&E-stained intestinal tissues from control group (**a**, **b**) and co-infection groups showing slight histopathological changes (**c, e, i, j**). Mild inflammation (**d**) mucosa is partly degenerated and sloughed off (**f**), mucosa-associated lymphoid tissue hyperplasia (**g**, **h**). Slightly increased vascularity in submucosa. Images were taken at 400× magnification. Scale bar = 25 µm

cholerae cells in the intestines was detected at 72 h post-infection. Interestingly, mild inflammation in the intestine was observed in the co-infection groups, potentially suggesting the presence of asymptomatic infection. Among them, significantly higher abundance of N16961 was detected in the faeces of mouse co-infected with ECOLI in comparison to that of EC at 24 h post-infection. Nonetheless, immunological response was largely similar across groups, except

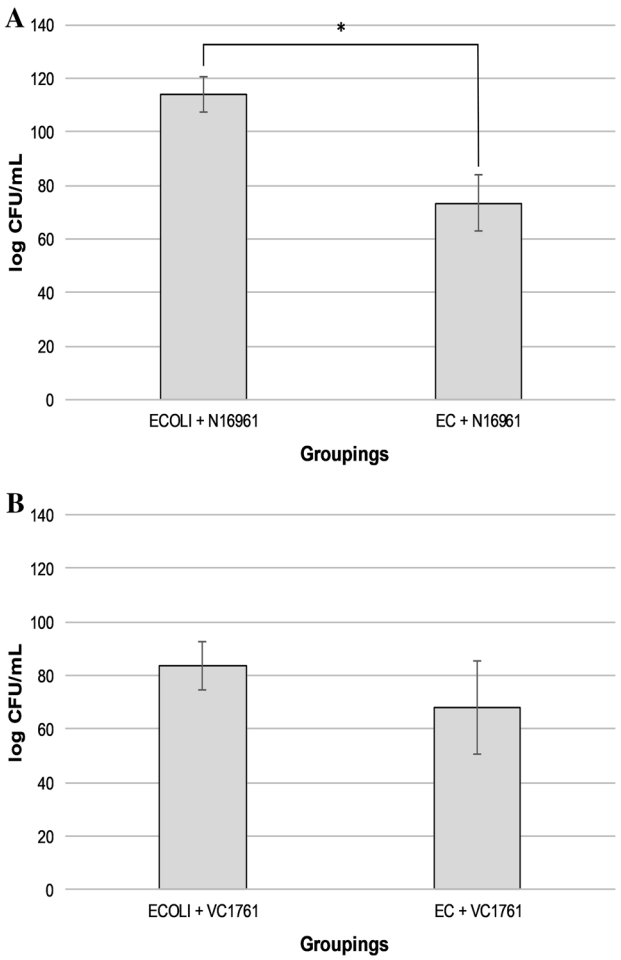

Fig. 6 Amount of *V. cholerae* detected in faecal samples after 24 h post-infection from **a** N16961 co-infection group, **b** VC1761 co-infection group. Data represent mean ± SE ($n = 6$ per group) from three independent experiments. Student's *t* test, $^*p < 0.05$

IL-5 and IL-10 which was upregulated in the *V. cholerae* (VC1761 and N16961) and ECOLI groups. A greater difference in AI-2 concentration was observed between the co-infection groups of N16961 (i.e. *E. coli* and *E. cloacae*) than the parallel groups for VC1761.

Evaluation of the adult mouse model

Several animal models have been used to study the disease progression of cholera [49]. Among them, the most established mouse model for *V. cholerae* infection is the infant mouse model, particularly in the study of growth and colonisation of *V. cholerae* in the intestine [50]. These experiments however, are often carried out in very short duration (e.g. < 24 h) as the infant mice usually displayed high mortality after removal from the mother [51–53]. In addition, the immune system and gut microbiota of the infant mice are still in the developmental stage, thus compromising the suitability of the model to represent actual infection in the complex system such as human gut [51–53].

It is notable that adult mouse model such as ligated ileal loops [3, 54] and the application of ketamine anaesthesia plus antibiotic treatment prior to infection [55] were previously proposed. However, both methods presented different technical challenges for the implementation.

Pathogenic *V. cholerae* including El Tor strains are known to harbour genes that encode for cholera toxin, an ADP-ribosylating protein enterotoxin [56]. Cholera toxin causes the influx of electrolytes and water into the intestinal lumen via the subsequent activation of adenylate cyclase and cystic fibrosis transmembrane conductance regulator (CFTR) [57, 58]. Overall, there were no significant differences in FA ratio between the control and co-infection groups upon termination of mice at 72 h post-infection. The fluid accumulation in ligated ileal loops of adult ICR outbred mice was found to achieve its maximal level at 12 h of *V. cholerae* incubation [3] and this is much earlier than our mice termination timeline. Therefore, the absence of fluid accumulation and symptomatic diarrhoea in mice was not unexpected. In addition, adult mice were previously reported to be less sensitive to the cholera toxin due to its expression of GM_1 ganglioside receptor [59].

It was previously shown that *V. cholerae* can still replicate and colonise the intestine of adult mouse despite showing little or no fluid accumulation at 16 h after intestinal inoculation [54]. Indeed, our qPCR results confirmed the presence of *V. cholerae* in the gastrointestinal tract of the experimental animals. The *ompW* signature was detectable in the faecal pellets of all the co-infection groups at 24 h, but the abundance dwindled over time and was below the detection limit in the faeces at 48 and 72 h post-infection. Nonetheless, using confocal microscopy, we detected the retention of small micro-colonies of *V. cholerae* cells in the intestine of all *V. cholerae*-infected mice. The result is consistent with the previous finding that *V. cholerae* are able to persist in the distal segment of small intestine of specific-pathogen-free mice for at least 72 h [55]. Taken together, our result suggests that the adult mice model can be used to monitor the transmission and colonisation of *V. cholerae*. It is noteworthy that eubacterial signals were observed despite antibiotic treatment. The presence of the commensals might contribute unknown effect in the experiment. For instance, microcolonies of yellow (commensals) and orange (*V. cholerae*), including those in peach, probably the mixture of both were observed (Fig. 4). Nonetheless, we assumed that the effects are equal across both single and co-infection models, and thus does not impact the validity of the comparison.

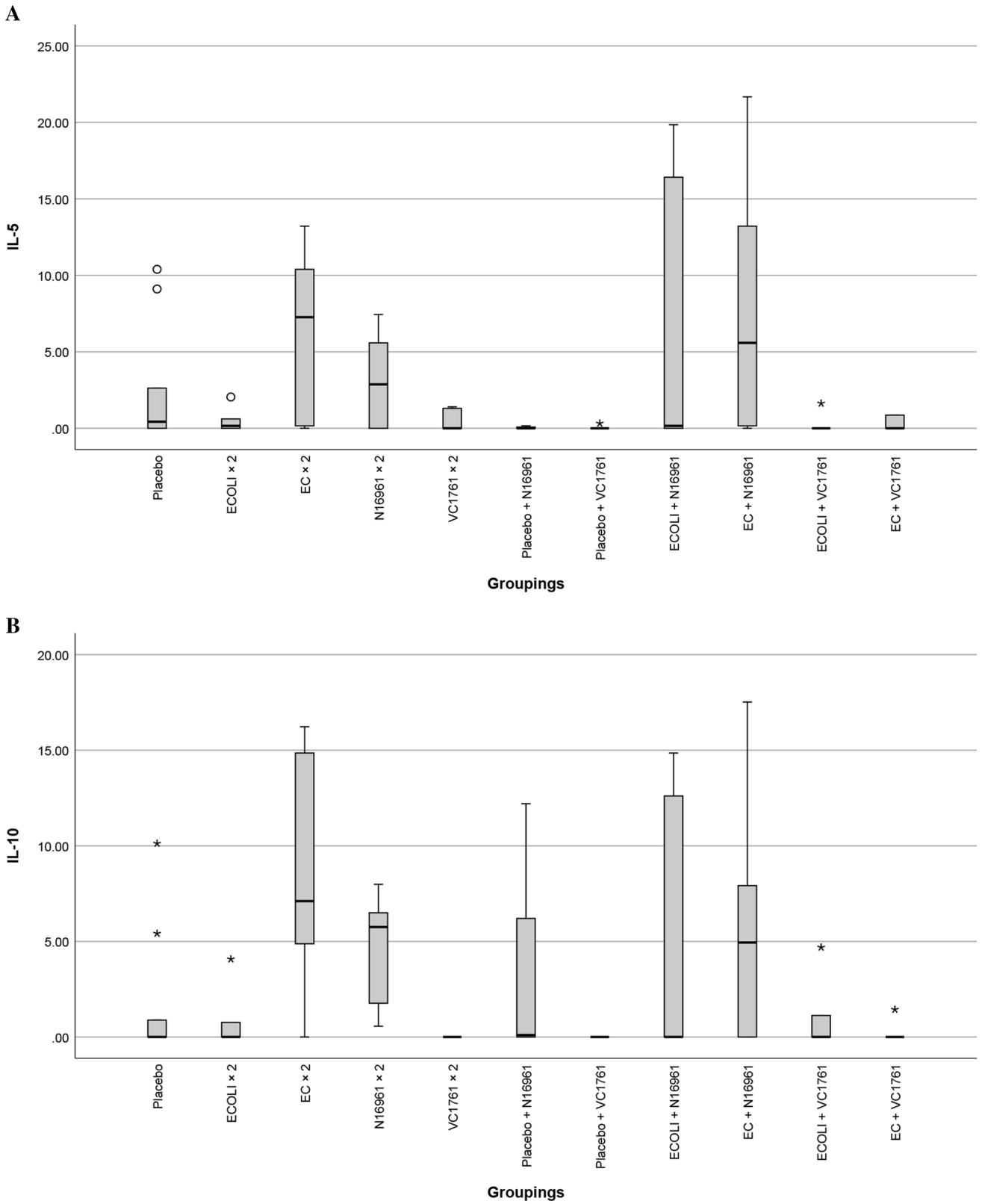

Fig. 7 Cytokine expression levels of **a** IL-5 and **b** IL-10 after 72 h of infection. The experiment was carried out in duplicates for each sample. Asterisks and dots represent outliers within each distribution

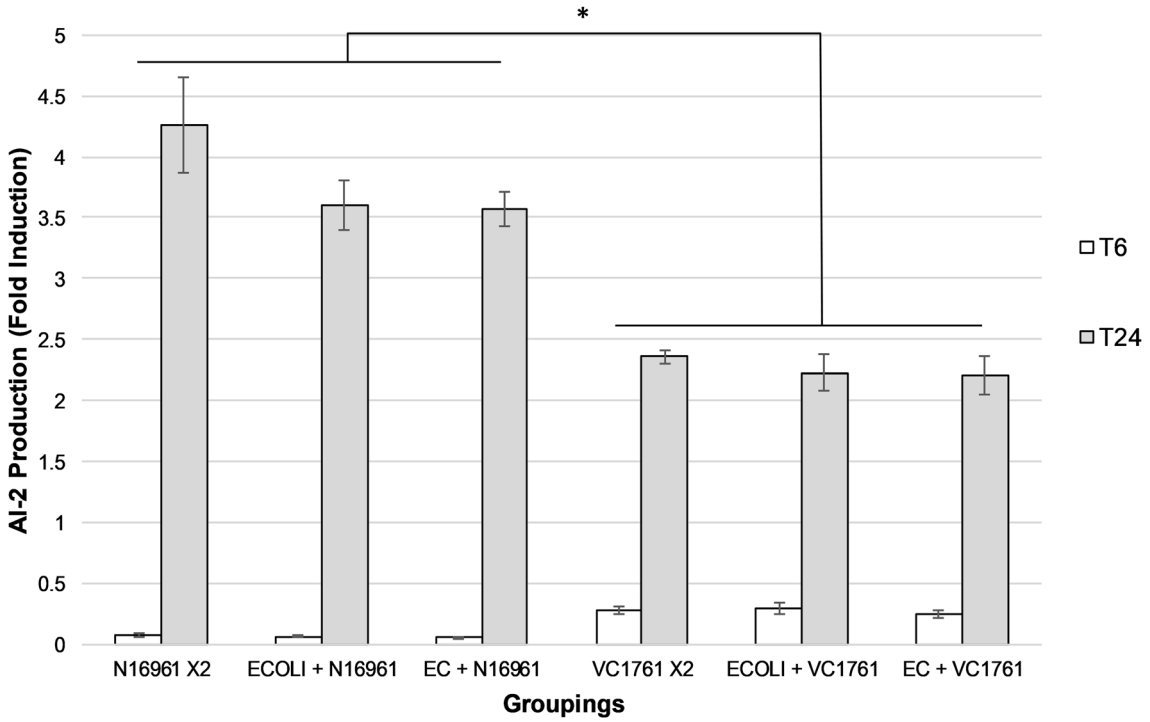

Fig. 8 Production of AI-2 from cell-free extracts from the control and co-infection groups during the 6- (T6) and 24-h (T24) measurement time points. Luminescence values are reported as the fold induction of luminescence by the *V. harveyi* BB170 reporter strain above the negative medium control. This figure represents mean ± SE from three independent experiments. Means with different letters are significantly different (Kruskal–Wallis test and pairwise comparisons with Bonferroni correction, $*p < 0.05$)

Histopathological changes in adult mouse model

In the aspect of histopathological changes, the sectioned distal intestinal segments of control groups consisting of only *V. cholerae* strains (N16961 and VC1761) showed no signs of inflammation in this study. The non- and minimal invasiveness of El Tor strains in causing marked inflammation of the intestinal epithelium in ligated rabbit ileal loop and cholera patients has been known previously [60, 61]. Interestingly, mild inflammation was observed in co-infection groups instead (but absent in EC and ECOLI), providing evidence on the potential role of coaggregation partnership in enhancing the pathogenicity of *V. cholerae*. Although it should be cautioned that *V. cholerae* uses T6SS secretion system to ablate competitors (in this case EC and ECOLI) which may also contribute to the observed inflammation. Histopathological changes such as partial degeneration of villous, dilated blood vessels and slight increase in vascularity of submucosa were observed. The severity comparison among the co-infection groups however, is not possible in this study due to the very minimal changes and lack of defined histomorphological scoring schemata for evaluation.

Recovery of *V. cholerae* cells from faecal pellets

One of the important aspects of infection other than successful intestinal colonisation is the ability of the pathogen to multiply and grow within the host prior to excretion back into the environment. For this reason, we monitored the amount of *V. cholerae* cells recovered from faecal pellets, as described in a previous study [62]. We found that at 24 h post-infection, both *V. cholerae* strains were detected in faecal pellets of single-species infection and co-infection arms. In the single-species infection, the detectable amount of N16961 was higher than VC1761 but not statistically significant. When N16961 were co-administered with ECOLI, the recovered *V. cholerae* cells were 40-fold significantly higher than that of EC. Although not statistically significant ($p > 0.05$), higher level of *V. cholerae* cells were detected in coaggregating partnership of VC1761 and ECOLI. This suggests the potential ability of *E. coli* in enhancing the replication and growth of *V. cholerae* within the gastrointestinal tract, and thus increased pathogenicity. Commensals were found to play an important role in host immunity [63, 64]. However, it was shown recently that

commensals may also promote the infection of virus and parasitic helminths in human host [65, 66].

At the later stage of infection, the detached *V. cholera*e from the small intestine will disseminate along the small intestine and excretion of *V. cholerae* either in the form of planktonic or biofilm-aggregates as cholera stool [67–71]. If this is the case, then we believe that the coaggregation partnership of *V. cholerae* with *E. coli* elicited better growth of *V. cholerae* can also contribute to the transmission and amplification of the cholera outbreak.

Immunological response

Marginally but statistically insignificant levels ($p > 0.05$) of IL-5 and IL-10 were found in the coaggregating ECOLI and *V. cholerae* than that of EC. The elevated levels of both cytokines indicate the activation of CD4 T helper 2 cells in response to cholera toxin prior to the enhancement of cytoplasmic cAMP [72]. IL-10 has also been shown to downregulate most cytokines produced by macrophages [73, 74], and as proposed by Olivier et al. [75], this could be aided by accessory toxins in El Tor O1 strains such as multifunctional autoprocessing RTX toxin (MARTX) and hemolysin, which in turn reduce the influx of phagocytic cells. This again explains the presence and persistence of *V. cholerae* cells in the intestines at 72 h post-infection.

Role of quorum sensing in *V. cholerae* pathogenicity

Quorum sensing via AI-2 signalling also allows the bacterial cells to monitor their population density and release necessary toxins or enzymes for survival, micro-colonies formation and dispersion for further colonisation [76]. At high cell density, AI-2 accumulates and activates the expression of the master quorum sensing HapR and HapA which represses the virulence gene expression and promote detachment of bacteria from intestine [77, 78]. In a recent study, Hay and Zhu reported that gut bacteria *Ruminococcus obeum* is able to restrict the colonisation of *V. cholerae* [79]. This particular bacterium prematurely induces *V. cholerae* quorum sensing by producing AI-2 and hence, represses the virulence and colonisation of *V. cholerae* in the gut [79]. The accumulation of AI-2 is also shown to negatively affect the biofilm formation and EPS biosynthesis [80]. As such, strong quorum sensing is expected to be reflected in high AI-2 concentration difference between the initiation (T6) and matured phase (T24) of the biofilm.

It is also notable that AI-2 production level in N16961 alone is significantly higher AI-2 than VC1761, suggesting stronger biofilm regulation via quorum sensing in N16961. This finding complemented our qPCR results where the coaggregating partnership of ECOLI with *V. cholerae* produced significantly higher levels of detectable quantities of *V. cholerae* cells recovered from faecal pellets at 24 h of infection. Nevertheless, the production of AI-2 is largely similar between the co-infection groups. The enhanced infectivity of the coaggregating partnership as reflected by the histopathological changes, bacterial cell density in faecal pellets and host immunological responses did not act through the quorum sensing system. The host inflammatory responses (intestinal inflammation and cytokines profile) could be triggered by high levels of cholera toxin in ECOLI and *V. cholerae* partnership, which then shifted the nutrient availability in the gut where more fluid such as electrolytes [81] and mucin [82] were secreted. The nutrient-rich fluid coincidentally produced an ideal growth medium for *V. cholerae* and the binding of *V. cholerae* to intestinal mucin by GbpA increased intestinal mucosal production which in turns favoured the adherence of more bacteria to the mucosa of small intestines as previously described by Bhowmick et al. [82]. While the production of AI-2 levels is taken into account in this study, the expression of HapR could further validate the current findings.

Overall differences in biofilm formation, pathogenicity and quorum sensing ability between *V. cholerae* El Tor and El Tor variant strains

We compared the Malaysian *V. cholerae* VC1761 with the wild-type strain N16961 in the aspects of their pathogenicity, quorum sensing and biofilm production. Both the pathogenicity (virulence gene expression) and biofilm production are centrally regulated by *HapR*. At high cell densities, the accumulation of CAI-1 autoinducer terminates small regulator RNA (sRNA) transcription and expression of HapR [83, 84]. HapR antagonistically decreases c-di-GMP pool which represses VpsT responsible in biofilm formation [85]. Additionally, HapR also represses the expression of AphA which downregulates virulence gene expression (*ctxA* and *tcpA*) [86]. Due to a frameshift mutation in *HapR* gene [77], the expression and downstream processes of HapR are disrupted. This may explain the higher colonisation observed in N16961 (than VC1761) which confer better survival within the host [77]. The *Hap*R mutation also suppresses HA protease that plays a role in cell detachment, as well as promoting the production of thick and densely packed biofilm [77]. As RNA extraction was not conducted in this study, the quantification of HapR and other quorum sensing gene expression (e.g. T6SS, CAI-1, etc.) was not possible. A separate study is required to understand the mechanism of interaction between *V. cholerae*, EC and ECOLI.

We speculated that EC might be competing for same niche in the host with N16961, resulting to lower cell count in the partnership of N16961 with EC than the partnership of N16961 with ECOLI. In contrast, low biofilm production exhibited by VC1761 may attributes to the natural response

of *HapR* to high cell density (*HapR* positive). Further, the general lower cell counts in the partnership of VC1761 with EC and ECOLI might be suggestive of competition. Such interaction may be comparable for phenotypically and genotypically similar strains.

In summary, we showed that the co-infection of *V. cholerae* with ECOLI and *V. cholerae* with EC were able to induce stronger histopathological response than both the tested *V. cholerae* strain alone in the intestine of adult mouse model. In addition, a stronger synergy was observed in the co-infection group of *V. cholerae* and ECOLI than *V. cholerae* and EC. Further investigation with different genotypes of *V. cholerae* strains is crucial to evaluate the presence of strains specific responses. In addition, parallel study that investigations the coaggregation relationship of *V. cholerae* with other important known commensals and probiotic cultures is warranted to determine the role of commensals in cholera development. From an applied perspective, the fundamental understanding of bacterial partners for the development of infection in this study may facilitate new prevention and treatment strategy for cholera.

Acknowledgements The authors would like to thank International Medical University and University of Malaya for providing the research facilities and instruments. The authors also thank two anonymous reviewers for their constructive comments to improve the manuscript.

Funding This study was supported by Fundamental Research Grant Scheme (FRGS), Ministry of Higher Education (MOHE).

Compliance with ethical standards

Conflict of interest The authors declare that they have no conflict of interest.

Ethical approval Animal experiments were conducted following the guidelines adapted from "Principle and Guide to Ethical Use of Laboratory Animals" by Ministry of Health Malaysia 2000. The study was approved by the Joint Committee on Research Ethics, International Medical University, Malaysia (IMU R 147/2014).

References

1. Gurbanov S, Akhmadov R, Shamkhalova G, Akhmadova S, Haley BJ, Colwell RR, Huq A (2011) Occurrence of *Vibrio cholerae* in municipal and natural waters and incidence of cholera in Azerbaijan. EcoHealth 8:468–477
2. Ali M, Nelson AR, Lopez AL, Sack DA (2015) Updated global burden of cholera in endemic countries. PLoS Negl Trop Dis 9:e0003832
3. Sawasvirojwong S, Srimanote P, Chatsudthipong V, Muanprasat C (2013) An adult mouse model of *Vibrio cholerae*-induced diarrhea for studying pathogenesis and potential therapy of cholera. PLoS Negl Trop Dis 7:e2293
4. Rothenbacher FP, Zhu J (2014) Efficient responses to host and bacterial signals during *Vibrio cholerae* colonization. Gut Microbes 5:120–128
5. Bart KJ, Huq Z, Khan M, Mosley WH (1970) Seroepidemiologic studies during a simultaneous epidemic of infection with El Tor Ogawa and classical Inaba *Vibrio cholerae*. J Infect Dis 121:S17–S24
6. Samadi A, Shahid N, Eusof A, Yunus M, Huq M, Khan M, Rahman A, Faruque A (1983) Classical *Vibrio cholerae* biotype displaces El Tor in Bangladesh. Lancet 1:805–807
7. Sack DA, Sack RB, Nair GB, Siddique AK (2004) Cholera. Lancet 363:223–233
8. Sack RB, Siddique AK, Longini IM Jr, Nizam A, Yunus M, Islam MS, Morris J, Glenn J, Ali A, Huq A, Nair GB (2003) A 4-year study of the epidemiology of *Vibrio cholerae* in four rural areas of Bangladesh. J Infect Dis 187:96–101
9. Khan M, Shahidullah M (1980) Cholera due to the El Tor biotype equals the classical biotype in severity and attack rates. J Trop Med Hyg 83:35–39
10. Niyogi S (1979) Studies on cholera carriers and their role in transmission of the infection: a preliminary report. Indian J Med Res 70:892–897
11. Woodward WE, Mosley WH (1972) The spectrum of cholera in rural Bangladesh II. Comparison of El Tor Ogawa and classical Inaba infection. Am J Epidemiol 96:342–351
12. Ang GY, Yu CY, Balqis K, Elina HT, Azura H, Hani MH, Yean CY (2010) Molecular evidence of cholera outbreak caused by a toxigenic *Vibrio cholerae* O1 El Tor variant strain in Kelantan, Malaysia. J Clin Microbiol 48:3963–3969
13. Teh CSJ, Suhaili Z, Lim KT, Khamaruddin MA, Yahya F, Sajili MH, Yeo CC, Thong KL (2012) Outbreak-associated *Vibrio cholerae* genotypes with identical pulsotypes, Malaysia, 2009. Emerg Infect Dis 18:1177–1179
14. Lee JH, Han KH, Choi SY, Lucas ME, Mondlane C, Ansaruzzaman M, Nair GB, Sack DA, von Seidlein L, Clemens JD (2006) Multilocus sequence typing (MLST) analysis of *Vibrio cholerae* O1 El Tor isolates from Mozambique that harbour the classical CTX prophage. J Med Microbiol 55:165–170
15. Nair GB, Faruque SM, Bhuiyan NA, Kamruzzaman M, Siddique AK, Sack DA (2002) New variants of *Vibrio cholerae* O1 biotype El Tor with attributes of the classical biotype from hospitalized patients with acute diarrhea in Bangladesh. J Clin Microbiol 40:3296–3299
16. Nair GB, Safa A, Bhuiyan N, Nusrin S, Murphy D, Nicol C, Valcanis M, Iddings S, Kubuabola I, Vally H (2006) Isolation of *Vibrio cholerae* O1 strains similar to pre-seventh pandemic El Tor strains during an outbreak of gastrointestinal disease in an island resort in Fiji. J Med Microbiol 55:1559–1562
17. Nguyen BM, Lee JH, Cuong NT, Choi SY, Hien NT, Anh DD, Lee HR, Ansaruzzaman M, Endtz HP, Chun J, Lopez AL, Czerkinsky C, Clemens JD, Kim DW (2009) Cholera outbreaks caused by an altered *Vibrio cholerae* O1 El Tor biotype strain producing classical cholera toxin B in Vietnam in 2007–2008. J Clin Microbiol 47:1568–1571
18. Ali A, Chen Y, Johnson JA, Redden E, Mayette Y, Rashid MH, Stine OC, Morris JG Jr (2011) Recent clonal origin of cholera in Haiti. Emerg Infect Dis 17:699–701
19. Ceccarelli D, Spagnoletti M, Cappuccinelli P, Burrus V, Colombo MM (2011) Origin of *Vibrio cholerae* in Haiti. Lancet Infect Dis 11:262
20. Ghosh-Banerjee J, Senoh M, Takahashi T, Hamabata T, Barman S, Koley H, Mukhopadhyay AK, Ramamurthy T, Chatterjee S, Asakura M, Yamasaki S, Nair GB, Takeda Y (2010) Cholera toxin production by the El Tor variant of *Vibrio cholerae* O1 compared to prototype El Tor and classical biotypes. J Clin Microbiol 48:4283–4286
21. Son MS, Megli CJ, Kovacikova G, Qadri F, Taylor RK (2011) Characterization of *Vibrio cholerae* O1 El Tor biotype variant clinical isolates from bangladesh and haiti, including a

molecular genetic analysis of virulence genes. J Clin Microbiol 49:3739–3749
22. Satitsri S, Pongkorpsakol P, Srimanote P, Chatsudthipong V, Muanprasat C (2016) Pathophysiological mechanisms of diarrhea caused by the *Vibrio cholerae* O1 El Tor variant: an in vivo study in mice. Virulence 7:789–805
23. Tamura K, Stecher G, Peterson D, Filipski A, Kumar S (2013) MEGA6: molecular evolutionary genetics analysis version 6.0. Mol Biol Evol 30:2725–2729
24. Malik A, Sakamoto M, Hanazaki S, Osawa M, Suzuki T, Tochigi M, Kakii K (2003) Coaggregation among nonflocculating bacteria isolated from activated sludge. Appl Environ Microbiol 69:6056–6063
25. Naves P, del Prado G, Huelves L, Gracia M, Ruiz V, Blanco J, Dahbi G, Blanco M, del Carmen Ponte M, Soriano F (2008) Correlation between virulence factors and in vitro biofilm formation by *Escherichia coli* strains. Microb Pathog 45:86–91
26. Galen JE, Ketley JM, Fasano A, Richardson SH, Wasserman SS, Kaper JB (1992) Role of *Vibrio cholerae* neuraminidase in the function of cholera toxin. Infect Immun 60:406–415
27. Halpern M, Landsberg O, Raats D, Rosenberg E (2007) Culturable and VBNC *Vibrio cholerae*: interactions with chironomid egg masses and their bacterial population. Microb Ecol 53:285–293
28. Heidelberg JF, Heidelberg KB, Colwell RR (2002) Bacteria of the gamma-subclass Proteobacteria associated with zooplankton in Chesapeake Bay. Appl Environ Microbiol 68:5498–5507
29. Nallabelli N, Patil PP, Pal VK, Singh N, Jain A, Patil PB, Grover V, Korpole S (2016) Biochemical and genome sequence analyses of *Megasphaera* sp. strain DISK18 from dental plaque of a healthy individual reveals commensal lifestyle. Sci Rep 6:33665
30. Zhou H, Wang G, Wu M, Xu W, Zhang X, Liu L (2018) Phenol removal performance and microbial community shift during pH shock in a moving bed biofilm reactor (MBBR). J Hazard Mater 351:71–79
31. Datta A, Stapleton F, Willcox MD (2018) Bacterial coaggregation and cohesion among isolates from contact lens cases. Invest Ophthalmol Vis Sci 59:2729–2735
32. Rickard AH, Leach SA, Buswell CM, High NJ, Handley PS (2000) Coaggregation between aquatic bacteria is mediated by specific-growth-phase-dependent lectin-saccharide interactions. Appl Environ Microbiol 66:431–434
33. Back C, Douglas S, Emerson J, Nobbs A, Jenkinson H (2015) Streptococcus gordonii DL 1 adhesin SspB V-region mediates coaggregation via receptor polysaccharide of Actinomyces oris T14V. Mol Oral Microbiol 30:411–424
34. Balakrishna A (2013) In vitro evaluation of adhesion and aggregation abilities of four potential probiotic strains isolated from guppy (*Poecilia reticulata*). Braz Arch Biol Technol 56:793–800
35. Ledder RG, Timperley AS, Friswell MK, Macfarlane S, McBain AJ (2008) Coaggregation between and among human intestinal and oral bacteria. FEMS Microbiol Ecol 66:630–636
36. Stevens MR, Luo TL, Vornhagen J, Jakubovics NS, Gilsdorf JR, Marrs CF, Møretrø T, Rickard AH (2015) Coaggregation occurs between microorganisms isolated from different environments. FEMS Microbiol Ecol 91:fiv123
37. Rickard AH, Leach SA, Hall LS, Buswell CM, High NJ, Handley PS (2002) Phylogenetic relationships and coaggregation ability of freshwater biofilm bacteria. Appl Environ Microbiol 68:3644–3650
38. Almagro-Moreno S, Pruss K, Taylor RK (2015) Intestinal colonization dynamics of *Vibrio cholerae*. PLoS Pathog 11:e1004787
39. Katharios-Lanwermeyer S, Xi C, Jakubovics N, Rickard A (2014) Mini-review: microbial coaggregation: ubiquity and implications for biofilm development. Biofouling 30:1235–1251
40. Min K, Zimmer M, Rickard A (2010) Physicochemical parameters influencing coaggregation between the freshwater bacteria *Sphingomonas natatoria* 2.1 and *Micrococcus luteus* 2.13. Biofouling 26:931–940
41. Khemaleelakul S, Baumgartner JC, Pruksakom S (2006) Autoaggregation and coaggregation of bacteria associated with acute endodontic infections. J Endod 32:312–318
42. Vornhagen J, Stevens M, McCormick DW, Dowd SE, Eisenberg JN, Boles BR, Rickard AH (2013) Coaggregation occurs amongst bacteria within and between biofilms in domestic showerheads. Biofouling 29:53–68
43. Burmølle M, Ren D, Bjarnsholt T, Sørensen SJ (2014) Interactions in multispecies biofilms: do they actually matter? Trends Microbiol 22:84–91
44. Bardill JP, Zhao X, Hammer BK (2011) The Vibrio cholerae quorum sensing response is mediated by Hfq-dependent sRNA/mRNA base pairing interactions. Mol Microbiol 80:1381–1394
45. Katzianer DS, Wang H, Carey RM, Zhu J (2015) "Quorum nonsensing": social cheating and deception in *Vibrio cholerae*. Appl Environ Microbiol 81:3856–3862
46. Ritchie JM, Rui H, Bronson RT, Waldor MK (2010) Back to the future: studying cholera pathogenesis using infant rabbits. mBio 1:e00047-10
47. Silva AJ, Benitez JA (2016) *Vibrio cholerae* biofilms and cholera pathogenesis. PLoS Negl Trop Dis 10:e0004330
48. Tamayo R, Patimalla B, Camilli A (2010) Growth in a biofilm induces a hyperinfectious phenotype in *Vibrio cholerae*. Infect Immun 78:3560–3569
49. Richardson SH (1994) Animal models in cholera research. In: Wachsmuth IK, Blake PA, Olsvik O (eds) *Vibrio cholerae* and cholera: molecular to global perspectives. ASM Press, Washington DC, pp 203–226
50. Herrington DA, Hall RH, Losonsky G, Mekalanos JJ, Taylor RK, Levine MM (1988) Toxin, toxin-coregulated pili, and the toxR regulon are essential for *Vibrio cholerae* pathogenesis in humans. J Exp Med 168:1487–1492
51. Darmoul D, Brown D, Selsted ME, Ouellette AJ (1997) Cryptdin gene expression in developing mouse small intestine. Am J Physiol 272:G197–206
52. Hermiston ML, Gordon JI (1995) Organization of the crypt-villus axis and evolution of its stem cell hierarchy during intestinal development. Am J Physiol 268:G813–822
53. Klose KE (2000) The suckling mouse model of cholera. Trends Microbiol 8:189–191
54. Basu S, Pickett MJ (1969) Reaction of *Vibrio cholerae* and choleragenic toxin in ileal loop of laboratory animals. J Bacteriol 100:1142–1143
55. Olivier V, Salzman NH, Satchell KJ (2007) Prolonged colonization of mice by *Vibrio cholerae* El Tor O1 depends on accessory toxins. Infect Immun 75:5043–5051
56. Hodges K, Gill R (2010) Infectious diarrhea: cellular and molecular mechanisms. Gut Microbes 1:4–21
57. Kaper J, Morris JJ, Levine M (1995) Cholera. Clin Microbiol Rev 8:48–86
58. Bharati K, Ganguly NK (2011) Cholera toxin: a paradigm of a multifunctional protein. Indian J Med Res 133:179–187
59. Richardson S, Sexton T, Rader J, Kajs C (1993) Biochemical and genetic basis for the ETS (enterotoxin sensitivity) phenotype in mice. Clin Infect Dis 16:S83–S91
60. Polotsky YE, Dragunskaya EM, Samostrelsky AY, Vasser NR, Efremov VE, Snigirevskaya ES, Seliverstova VG (1977) Interaction of *Vibrio cholerae* El Tor and gut mucosa in ligated rabbit ileal loop experiment. Med Biol 55:130–140
61. Qadri F, Bhuiyan TR, Dutta KK, Raqib R, Alam MS, Alam NH, Svennerholm AM, Mathan MM (2004) Acute dehydrating disease caused by *Vibrio cholerae* serogroups O1 and O139 induce increases in innate cells and inflammatory mediators at the mucosal surface of the gut. Gut 53:62–69

62. Nygren E, Li BL, Holmgren J, Attridge SR (2009) Establishment of an adult mouse model for direct evaluation of the efficacy of vaccines against *Vibrio cholerae*. Infect Immun 77:3475–3484
63. Round JL, Mazmanian SK (2009) The gut microbiota shapes intestinal immune responses during health and disease. Nat Rev Immunol 9:313
64. Belkaid Y, Hand TW (2014) Role of the microbiota in immunity and inflammation. Cell 157:121–141
65. Kuss SK, Best GT, Etheredge CA, Pruijssers AJ, Frierson JM, Hooper LV, Dermody TS, Pfeiffer JK (2011) Intestinal microbiota promote enteric virus replication and systemic pathogenesis. Science 334:249–252
66. Reynolds Lisa A, Smith Katherine A, Filbey Kara J, Harcus Yvonne, Hewitson James P, Redpath Stephen A, Valdez Yanet, Yebra María J, Brett Finlay B, Maizels Rick M (2014) Commensal–pathogen interactions in the intestinal tract. Gut Microbes 5:522–532
67. Wang H, Ayala JC, Benitez JA, Silva AJ (2012) Interaction of the histone-like nucleoid structuring protein and the general stress response regulator RpoS at *Vibrio cholerae* promoters that regulate motility and hemagglutinin/protease expression. J Bacteriol 194:1205–1215
68. Wang H, Ayala JC, Benitez JA, Silva AJ (2014) The LuxR-type regulator VpsT negatively controls the transcription of rpoS, encoding the general stress response regulator, in *Vibrio cholerae* biofilms. J Bacteriol 196:1020–1030
69. Nielsen AT, Dolganov NA, Otto G, Miller MC, Wu CY, Schoolnik GK (2006) RpoS controls the *Vibrio cholerae* mucosal escape response. PLoS Pathog 2:e109
70. Silva AJ, Sultan SZ, Liang W, Benitez JA (2008) Role of the histone-like nucleoid structuring protein in the regulation of rpoS and RpoS-dependent genes in *Vibrio cholerae*. J Bacteriol 190:7335–7345
71. Nelson EJ, Harris JB, Morris JG, Calderwood SB, Camilli A (2009) Cholera transmission: the host, pathogen and bacteriophage dynamic. Nat Rev Microbiol 7:693–702
72. Yamamoto M, Vancott JL, Okahashi N, Marinaro M, Kiyono H, Fujihashi K, Jackson RJ, Chatfield SN, Bluethmann H, McGHEE JR (1996) The role of Th1 and Th2 cells for mucosal IgA responses. Ann N Y Acad Sci 778:64–71
73. Kambayashi T, Jacob CO, Zhou D, Mazurek N, Fong M, Strassmann G (1995) Cyclic nucleotide phosphodiesterase type IV participates in the regulation of IL-10 and in the subsequent inhibition of TNF-alpha and IL-6 release by endotoxin-stimulated macrophages. J Immunol 155:4909–4916
74. de Waal Malefyt R, Abrams J, Bennett B, Figdor CG, de Vries JE (1991) Interleukin 10(IL-10) inhibits cytokine synthesis by human monocytes: an autoregulatory role of IL-10 produced by monocytes. J Exp Med 174:1209–1220
75. Olivier V, Queen J, Satchell KJ (2009) Successful small intestine colonization of adult mice by *Vibrio cholerae* requires ketamine anesthesia and accessory toxins. PLoS One 4:e7352
76. Swift S, Vaughan EE, de Vos WM (2000) Quorum sensing within the gut ecosystem. Microb Ecol Health Dis 12:81–92
77. Zhu J, Miller MB, Vance RE, Dziejman M, Bassler BL, Mekalanos JJ (2002) Quorum-sensing regulators control virulence gene expression in *Vibrio cholerae*. Proc Natl Acad Sci USA 99:3129–3134
78. Singh PK, Bartalomej S, Hartmann R, Jeckel H, Vidakovic L, Nadell CD, Drescher K (2017) *Vibrio cholerae* combines individual and collective sensing to trigger biofilm dispersal. Curr Biol 27:3359–3366.e7
79. Hay A, Zhu J (2014) Microbiota talks cholera out of the gut. Cell Host Microbe 16:549–550
80. Ali SA, Benitez JA (2009) Differential response of *Vibrio cholerae* planktonic and biofilm cells to autoinducer 2 deficiency. Microbiol Immunol 53:582–586
81. Hase CC, Mekalanos JJ (1999) Effects of changes in membrane sodium flux on virulence gene expression in *Vibrio cholerae*. Proc Natl Acad Sci USA 96:3183–3187
82. Bhowmick R, Ghosal A, Das B, Koley H, Saha DR, Ganguly S, Nandy RK, Bhadra RK, Chatterjee NS (2008) Intestinal adherence of *Vibrio cholerae* involves a coordinated interaction between colonization factor GbpA and mucin. Infect Immun 76:4968–4977
83. Rutherford ST, van Kessel JC, Shao Y, Bassler BL (2011) AphA and LuxR/HapR reciprocally control quorum sensing in vibrios. Genes Dev 25:397–408
84. Lenz DH, Mok KC, Lilley BN, Kulkarni RV, Wingreen NS, Bassler BL (2004) The small RNA chaperone hfq and multiple small RNAs control quorum sensing in *Vibrio harveyi* and *Vibrio cholerae*. Cell 118:69–82
85. Waters CM, Lu W, Rabinowitz JD, Bassler BL (2008) Quorum sensing controls biofilm formation in *Vibrio cholerae* through modulation of cyclic di-GMP levels and repression of vpsT. J Bacteriol 190:2527–2536
86. Kovacikova G, Skorupski K (2002) Regulation of virulence gene expression in *Vibrio cholerae* by quorum sensing: hapR functions at the aphA promoter. Mol Microbiol 46:1135–1147
87. Niu C, Gilbert ES (2004) Colorimetric method for identifying plant essential oil components that affect biofilm formation and structure. Appl Environ Microbiol 70:6951–6956
88. Naves P, del Prado G, Huelves L, Gracia M, Ruiz V, Blanco J, Rodrguez-Cerrato V, Ponte M, Soriano F (2008) Measurement of biofilm formation by clinical isolates of *Escherichia coli* is method-dependent. J Appl Microbiol 105:585–590